Environmental Advances 21 (2025) 100655

Contents lists available at ScienceDirect

Environmental Advances

journal homepage: www.sciencedirect.com/journal/environmental-advances

Human adipose tissue gene expression signatures indicate an inflammatory response and retinoic receptor activation under persistent organic pollutants exposure

Tobias Hagemann [a], Ulrike Rolle-Kampczyk [b], Kristin Schubert [b], Arne Dietrich [c], Martin von Bergen [b,d], Matthias Blüher [a,e,f], Anne Hoffmann [a,*]

[a] Helmholtz Institute for Metabolic, Obesity and Vascular Research (HI-MAG) of the Helmholtz Zentrum München at the University of Leipzig and University Hospital Leipzig, Leipzig, Germany
[b] Helmholtz-Centre for Environmental Research - UFZ, Department of Molecular Systems Biology, Leipzig, Germany
[c] Department for Visceral, Transplantation, Thoracic and Vascular Surgery, Leipzig University Hospital, Leipzig, Germany
[d] University of Leipzig, Institute of Biochemistry, Leipzig, Germany
[e] Divisions of Endocrinology and Nephrology, Leipzig University Medical Center, University of Leipzig, Leipzig, Germany
[f] German Center for Diabetes Research, Neuherberg, Germany

ARTICLE INFO

Keywords:
Persistent organic pollutants
Adipose tissue dysfunction
Gene expression
Obesity

ABSTRACT

Adipose tissue (AT) is subject to permanent accumulation of persistent organic pollutants (POP) due to their hydrophobic nature. Therefore, AT can be considered as interface between the body and an increasingly complex exposure to the chemical environment. As endocrinologically activate tissue, AT itself secretes adipokines regulating inflammation, insulin sensitivity and energy expenditure among others which are known to be dysfunctional in obesity. This study examined the impact of accumulated POPs 4,4-Diisoopropylbiphenyl (DIPB) and Ethyltetradecanoate (ETD) on human AT function. RNA-sequencing based gene expression analysis was conducted within the Leipzig Obesity Biobank (LOBB) between individuals ($N = 43$) with positive concentrations of DIPB and ETD in body fat against negative controls in subcutaneous (SAT) and visceral AT (VAT) in a sex-specific manner independent of their obesity status. Our study reveals sex- and AT-depot-specific gene expression profiles associated with immune responses, NF-κB signaling, and PPARγ pathways, highlighting POP interaction with immunological reactions in AT independent of obesity. Notably, our findings suggest altered retinoid acid receptor activity, which may influence AT browning. This research provides novel insights into the molecular mechanisms underlying the impact of POP exposure on human AT function. Importantly, our results indicate that POP exposure can contribute to AT dysfunction independently of obesity, suggesting that external environmental factors, such as POPs, should be considered as potential drivers of AT dysfunction in future obesity-related studies.

Introduction

The ongoing global increase in obesity prevalence remains a health burden to societies across continents (Worldwide trends in body-mass index, 2017). Obesity is associated with disorders like systemic inflammation (Rodríguez-Hernández et al., 2013), insulin resistance (Wilcox, 2005), type 2 diabetes (T2D) (Mokdad et al., 2003), and cardiovascular diseases (Ortega et al., 2016) and is a risk factor for severe courses or early onset of chronic diseases including rheumatoid arthritis (Crowson et al., 2013) and Alzheimer's disease (Rohm et al., 2022;

Abbreviations: AT, adipose tissue; DEG, Differentially expressed genes; DIPB, 4,4-Diisoopropylbiphenyl; ETD, Ethyltetradecanoate; FDR, false discovery rate; fT3, free Triiodothyronine; fT4, free Thyroxine; GC-MS, Gas chromatography-mass spectrometry; MHO, metabolically healthy obesity; NF-κB, nuclear factor-κB; PE, Pair-End; PPARγ, peroxisome proliferator-activated receptor gamma; POP, persistent organic pollutant; RA, retonoid acid; RAR, retinoid acid receptor; RNA-Seq, RNA-sequencing; RXR, retinoic X receptor; SAT, subcutaneous adipose tissue; T2D, type 2 diabetes; UCP-1, uncoupling protein-1; VAT, visceral adipose tissue.

* Corresponding author at: Helmholtz Institute for Metabolic, Obesity and Vascular Research (HI-MAG), Helmholtz Zentrum München at the University of Leipzig and University Hospital Leipzig, Philipp-Rosenthal-Straße 27, D-04103 Leipzig, Germany.
E-mail address: anne.hoffmann@helmholtz-munich.de (A. Hoffmann).

https://doi.org/10.1016/j.envadv.2025.100655
Received 10 March 2025; Received in revised form 13 June 2025; Accepted 26 June 2025
Available online 28 June 2025

Flores-Cordero et al., 2022).

Adipose tissue (AT) may link the obesogenic environment, changes in food intake and food contaminants to obesity and non-communicable diseases. Previously thought to act as a storage tissue, AT has proven to also have endocrine and metabolic functions, secreting numerous adipokines involved in the regulation of inflammation, insulin sensitivity, energy expenditure, glucose and lipid metabolism, and modulation of the immune system (Kershaw and Flier, 2004; Lehr et al., 2012; Fasshauer and Blüher, 2015). In many people living with obesity, AT function is impaired (Blüher, 2009) and AT dysfunction contributes to obesity related metabolic diseases (Blüher, 2013).

AT may be considered as interface between the body and an increasingly complex exposure to the chemical environment that include xenobiotics. In an organism, the majority of absorbed xenobiotic substances with potentially toxic function are subject to chemical manipulation through the xenobiotic metabolizing system (Barouki, 2010). However, the xenobiotic class of persistent organic pollutants (POP) is environmentally and biologically persistent and tends to accumulate in AT due to its hydrophobic nature (Fisher, 1999; Lee et al., 2014). Consequently, AT plays a significant role in the organism's response to acute POP exposure (La Merrill et al., 2013). By absorbing lipophilic chemicals, AT shifts POP bioaccumulation distribution in the body and safeguards other organs from direct exposure.

Considering that AT dysfunction contributes to systemic disorders related to increased (obesity) or significantly reduced subcutaneous (lipodystrophy) fat mass, it is important to investigate whether exposure to POPs affects adipose tissue function. As an example, exposure and bioaccumulation of POPs may contribute to impaired AT function and could play a role in the distinction between metabolically unhealthy and metabolically healthy obesity (MHO). MHO, although lacking a universally accepted definition, is generally characterized by an obese phenotype in conjunction with normal glucose and lipid metabolism parameters, as well as a significantly lower risk of developing cardiovascular diseases than individuals with metabolically unhealthy obesity (Blüher, 2020). Indeed, published data shows that lower POP levels in serum are associated with the MHO phenotype (Gauthier et al., 2014). In a previous study, we investigated POP accumulation in subcutaneous AT (SAT) and visceral AT (VAT) and found significant correlations between distinct POP AT concentrations and parameters of insulin sensitivity, fasting and chronic hyperglycemia in a sex and AT depot specific manner (Rolle-Kampczyk et al., 2020). Higher glucose parameters were associated with accumulation of POPs including 4,4-Diisopropylbiphenyl (DIPB) and Ethyltetradecanoate (ETD) suggesting a negative effect of POPs on glucose metabolism. Moreover, DIPB and ETD levels in AT have shown significant correlations with the number of macrophages in AT (Rolle-Kampczyk et al., 2020) as indicator of tissue inflammation and dysregulation. However, there is a lack of coverage of both compounds in the literature especially in context of adipose tissue accumulation and the molecular mechanisms for the observed associations are unclear.

In the present study, we aim to investigate underlying mechanisms which cause alterations in AT function under conditions of high DIPB and ETD exposure. While many of the covered POPs in the previous study are detected throughout the study cohort, both DIPB and ETD signals in the POP data provide control samples without accumulation of any of both POPs which are suitable for a differential approach. We added information from bulk SAT and VAT RNA-sequencing (RNA-Seq) data to the previously analyzed cohort (Rolle-Kampczyk et al., 2020) and analyzed gene expression differences between AT from individuals with and without DIPB and ETD accumulation. Since POP effects on parameters of AT function and systemic metabolism have been shown to be specific to AT depots and sex, we considered VAT and SAT as well as women and men individually.

Material and methods

Cohort characteristics

We selected 43 AT donors from the cross-sectional cohort of the Leipzig Obesity BioBank (LOBB; https://www.helmholtz-munich.de/en/hi-mag/cohort/leipzig-obesity-bio-bank-lobb) initially utilized in our previous study (Rolle-Kampczyk et al., 2020), where sufficient quantities of abdominal SAT and omental VAT samples were available, along with high-quality RNA sequencing data. Based on this cohort, 43 AT donors were selected where SAT and VAT samples were available in sufficient amounts and with high quality RNA-Seq data. The studied population includes both women ($N = 22$; mean age = 64.83 ± 12.34 years; mean BMI = 29.22 ± 11.13 kg/m^2; 18.2 % T2D) and men ($N = 21$; mean age = 64.77 ± 14.55 years; mean BMI = 30.06 ± 6.14 kg/m^2; 23.8 % T2D). Detailed cohort characteristics are shown in Suppl. Table 1. Adipose tissue biopsies were collected during elective laparoscopic abdominal surgery between 2008 and 2018, as previously described (Langhardt et al., 2018), from individuals who underwent abdominal surgery for cholecystectomy, weight reduction surgery, or explorative laparotomy. Shortly before the operation, body composition measurements were conducted and blood samples were collected to assess metabolic parameters, in accordance with current protocols (Klöting et al., 2010). Exclusion criteria included chronic substance or alcohol misuse, smoking within the 12 months prior to surgery, acute inflammatory diseases, use of glitazones as concomitant medication, end-stage malignant diseases, weight loss exceeding 3 % in the three months preceding surgery, uncontrolled thyroid disorder, and Cushing's disease.

Measurement of POPs in adipose tissue

Sample preparation and gas chromatography-mass spectrometry (GC-MS) measurement of persistent organic pollutants (POPs) was performed as previously described (Rolle-Kampczyk et al., 2020). Briefly, 250 mg lipid tissue were homogenized multiple times, spiked with internal standard (PCB 116-d5 and α-HCH-D6) and sample extract was combined with DDT-D8 (qualifier) in a GC-vial. The GC-MS analyses of the prepared fat samples were performed using the 7890A GC system coupled to the 5975C inert XL MSD with Triple-Axis Detector (both Agilent Technologies, Santa Clara, USA). In the GC set-up, an Optima 5MS (30 m × 250 μm × 0.25 μm, Macherey-Nagel, Düren, Germany) column and a Backflush Transfer column (1 m × 100 μm × 0 μm, Agilent Technologies) were applied. The identification was done by NIST library (Version 2011). The peak intensities were normalized by dividing the contaminants' peak intensity by the peak intensity of the spiked internal standard in the sample and then multiplying by the median of the peak intensities from the spike-in standard across all samples. Ethyltetradecanoate and 4,4-Diisopropylbiphenyl were chosen from the pool of POPs because a substantial number of negative control samples are available for these compounds which is crucial for ensuring the interpretability of the results in differential gene expression analysis.

Patient group allocation based on pollutant bioaccumulation

Pollutant exposure groups were defined as controls and positives based on having GC-MS measurements of the respective POP equal to zero or larger than zero, respectively. For DIPB, this resulted in $N = 12$ controls ($N_{women} = 6$) and $N = 25$ positives ($N_{women} = 14$) in SAT and $N = 9$ controls ($N_{women} = 4$) and $N = 23$ positives ($N_{women} = 11$) in VAT. For ETD, $N = 16$ controls ($N_{women} = 10$) and $N = 21$ positives ($N_{women} = 10$) were found in SAT and $N = 8$ controls ($N_{women} = 5$) and $N = 24$ positives ($N_{women} = 10$) in VAT (Suppl. Figure 1).

RNA-sequencing of adipose tissue

RNA extraction of frozen tissues was performed using the RNeasy Mini lipid kit (Qiagen Ltd, Germantown, MD, USA). RNA samples were quantified using Qubit 4.0 Fluorometer (Life Technologies, Carlsbad, CA, USA) and RNA integrity was checked with RNA Kit on Agilent 5600 Fragment Analyzer (Agilent Technologies, Palo Alto, CA, USA). The polyA-selected RNA-Seq libraries were generated with the NEBNext Ultra II Directional RNA Library Prep Kit for Illumina as per the manufacturer's instructions (NEB in Ipswich, MA, USA). Validation of the sequencing libraries was performed using the DNA Kit on the Agilent 5600 Fragment Analyzer (Agilent Technologies, Palo Alto, CA, USA), and quantification was carried out using the Qubit 4.0 Fluorometer (Invitrogen, Carlsbad, CA, USA). Subsequently, the libraries were multiplexed and loaded onto the flow cell of an Illumina NovaSeq 6000 instrument following the manufacturer's protocol. The samples underwent sequencing in a 2 × 150 Pair-End (PE) configuration v1.5. Image analysis and base calling were conducted by the NovaSeq Control Software v1.7 on the NovaSeq platform by the Leipzig laboratory of GENEWIZ Germany GmbH. In total, $N = 69$ RNA-Seq samples from the 43 patients were collected originating from SAT ($N_{women} = 20$; $N_{men} = 17$) and VAT ($N_{women} = 15$; $N_{men} = 17$).

RNA-sequencing data preprocessing

Adapter trimmed and quality-filtered RNA sequencing reads were aligned against the human genome assembly GRCh38.p13 (Schneider et al., 2017) (hg38) using STAR aligner (Dobin et al., 2013) (v.2.7.8a) with a maximum of 50 multiple alignments per read. FeatureCounts (Liao et al., 2014) (v2.0.1) was used to assign genomic features to mapped reads, where duplicated reads were ignored and multiple mapped reads were counted fractionally. The quality of each step was ensured using FASTQC (Babraham Bioinformatics) (v.0.11.4).

Gene count matrices were preprocessed individually for each tissue and sex combination. Data homoscedastic normalization with respect to library size was performed using the variance stabilizing transformation from the R package DESeq2 (Michael Love, 2017) (v1.42.1) and only genes with a normalized mean count > 10 were kept. Next, we accounted for biological bias and technical artifacts in the data, which otherwise can introduce significant variance in the expression data and potentially mask subtler pollutant-induced gene expression changes. For this purpose, the sva package (Leek et al., 2019) (v3.50) was employed. In brief, the subset of data is identified which is exclusively influenced by artifacts and subsequently estimated as surrogate variable by matrix decomposition. For this purpose, the *svaseq* function (Leek, 2014) was applied to compute the first five surrogate variables in the gene expression data given the contrast between positive and control samples. Unwanted variance was removed from the expression data with the *removeBatchEffect* function from the R package limma (Ritchie et al., 2015) (v3.58.1) with covariates age, BMI and previously computed first five surrogate variables. We did not adjust for other pollutants, as no consistent or systematic influence was observed. Adjusting for minor effects could have unnecessarily attenuated the true biological signals and compromise the interpretability of the results. Subsequently, the *prince* function from the swamp (Leek, 2014) (v1.5.1) R package was used to test, if the first principal components (PC) of the adjusted expression data showed any associations with the POP groups in a linear regression model. Examination of gene expression data after dimension reduction showed that the inclusion of surrogate variables and covariates age and BMI in the models successfully removed not only batch effects but also gives emphasize on the contrast between positive and control groups for POP exposure (as shown in the result section). This demonstrates the discriminative power of the provided parameters giving a solid foundation for subsequent differential analysis of gene expression signal.

Differential gene expression analysis

Differential gene expression analysis was performed using DESeq2. In brief, DESeq2 fits a linear model to model the gene counts while taking variability of genes and library size factor of biological replicates into account. Here, a linear model design was applied including age, BMI and the first five surrogate variables as covariates as well as the contrast between pollutant exposure groups. Differentially expressed genes (DEG) with a false discovery rate (FDR) adjusted p-value <0.05 are considered as statistically significant.

Gene network and enrichment analysis

For characterization of sets of DEGs, gene network analysis was conducted with the web interface of the STRING database (Szklarczyk et al., 2023) (v12.0; accessed on 28th June 2024) to find associations and interactions of DEGs on protein level and add context to the regulated genes with regard to the gene product after translation. Functional analysis of DEGs was performed using QIAGEN Ingenuity Pathway Analysis (IPA) software (QIAGEN Inc., https://digitalinsights.qiagen.com/IPA) (Krämer et al., 2014) to identify genes that are over-represented or underrepresented in specific gene sets, providing insight into the functional impact of changes in gene expression. This analysis leverages IPA's comprehensive catalogs for diseases and biological functions, as well as its tox functions catalog, which annotates genes associated with toxicity endpoints and phenotypes. In this knowledge-based approach, IPA provides curated sets of genes and utilizes Fisher's exact test to infer, which gene sets are significantly enriched in the list of DEGs. Notably, this analysis does not account for the direction of expression changes, as the effects of POP on gene expression are expected to be complex and potentially arbitrary. As these effects are often modest, unadjusted p-values are displayed for enrichment results to avoid over-correction and increase the sensitivity of the analysis. Additionally, gene set enrichment analysis was performed with the enrichR R package (Jawaid, 2023; Chen et al., 2013) (v3.2) querying the Kyoto Encyclopedia of Genes and Genomes (KEGG, 2021) (Kanehisa et al., 2016) and Reactome (2022) (Croft et al., 2011) database. The two independent enrichment tools enrichR and IPA are applied to extend and validate result of each enrichment approach.

Statistical analysis

Analyses were performed under R version 4.3.2. Correlations were computed with the psych R package (Imai et al., 2010) (v2.4.3) using Spearman's correlation with 95 % confidence interval. P-values are reported without adjustment as no correlation remained significant after correction for multiple testing.

Results

Differential gene expression is related to 4,4-Diisopropylbiphenyl (DIBP) accumulation

First, we performed differential gene expression analysis in respect to DIBP exposure signal derived from previous data (Rolle-Kampczyk et al., 2020). Availability for gene expression data and DIBP measurements in the cohort yielded $N = 37$ samples in SAT ($N_{women} = 20$; $N_{men} = 17$) and $N = 27$ samples in VAT ($N_{women} = 15$; $N_{men} = 17$). AT depots displayed distinct distributions of DIPB accumulation, leading to the establishment of separate control groups for each depot. Consequently, the data from each depot was analyzed separately. An overview of the workflow is given in Suppl. Figure 2. After adjustment of gene transcription data for strong sources of variance (as described above), dimension reduction with principal component (PC) analysis of gene transcription data achieves separation of DIPB positive samples and controls by the first two PCs (Suppl. Figure 3). The first PC is significantly associated with the

contrast of the DIPB group in both AT depots and sex groups. Differential gene expression analysis for DIPB exposure in SAT revealed sex-specific associations. A total of four genes were significantly upregulated in DIPB positive women in contrast to women in the control group including *PPARG, MT1X, SPSB1* and *PLXNB3* as shown in Fig. 1A-B and Suppl. Table 2A. None of the above genes were found among the significant DEGs in men. In SAT from men, *ITGA5* was the only DEG being downregulated in the positive group (Fig. 1C-D, Suppl. Table 3A). Ingenuity Pathways Analysis (IPA) for biological functions highlights affiliation to inflammatory response, dysfunctions and abnormalities to *PPARG* (e.g. cytopenia, proliferation of endothelial cells, apoptosis and obesity; Suppl. Table 2C) and *ITGA5* (e.g. rheumatoid arthritis and anemia; Suppl. Table 3C).

We repeated the sex-specific DEG analysis of expression data between DIPB bioaccumulation groups in VAT ($N_{women} = 15$; $N_{men} = 17$). In VAT from women, *MICA, NPHS1, ADAM33* and *TEDC1* were differentially expressed (Fig. 1E-F; Suppl. Table 4A). Enrichment through IPA reveals associations with immunological diseases for *MICA* (e.g. celiac disease; Suppl. Table 4C). In VAT from men, the set of DEGs encompasses the biological processes of cell signaling and metabolism, as well as immune response functions, notably *IDO1, LYZ, FCER1G*, and *CD84*, which are involved in modulating immune cell interactions and inflammation. (Fig. 1G-H, Suppl. Table 5A). Overall, DEGs are enriched for inflammatory responses and abnormalities with regard to biological functions (e.g. cell viability, cell proliferation of T lymphocytes; Suppl. Table 5C). On protein level, StringDB network analysis clusters DEGs based on predicted coexpression interaction where genes *LYZ, FCER1G, NCKAP1L, CTSS* and *CTSZ* are significantly enriched for neutrophile degranulation (Suppl. Figure 4).

Notably, individual DEGs exhibited no overlap between men and women, nor between AT depots, across all tested subgroups. Furthermore, the incorporation of clinical phenotype parameters reveals that DIPB is specifically correlated with free Thyroxine (fT4) in SAT from women and VAT from men. This correlation is further supported by similar associations of DEGs in each subgroup. In contrast, DIPB accumulation is associated with cholesterol in male SAT and female VAT, although the corresponding DEG signals are only observed by *ITGA5* in male SAT (Fig. 2, Suppl. Tables 4D, 5D).

Differential gene expression is associated with Ethyltetradecanoate (ETD) accumulation

In parallel to our evaluation of DIPB, gene expression signal analysis was conducted with respect to ETD exposure similar to the evaluation described for DIPB. In total, available data covers $N = 37$ samples in SAT ($N_{women} = 20$; $N_{men} = 17$) and $N = 32$ in VAT ($N_{women} = 15$; $N_{men} = 17$). Dimensional reduction with PCA achieved a separation of ETD groups by the first two PCs in all sex groups and AT depots. In all tested conditions, the first PC is significantly associated with ETD AT exposure (Suppl. Figure 5). Differentially expressed genes in SAT from women for the contrast of positive and control samples for ETD accumulation cover cell signaling processes and particularly *CARD10, HLA-DRB1* and *CYSLTR1* which are involved in immune response activity (Fig. 3A-B; Suppl. Table 6A). Enrichment with IPA for diseases and biological functions highlights immune response effects in SAT from women, e.g. T cell activation and proliferation (*HLA-DRB1*; Suppl. Table 6C). When comparing normalized expression signal of DEGs with anthropometric parameters via Spearman's correlation, a systematic association is found for adiponectin in SAT from women including *CARD10*, which is supported by significant correlation of ETD accumulation with adiponectin (Fig. 4, Suppl. Table 6D). In SAT from men, ETD accumulation groups are associated with a variety of DEGs including *MMP9* (Fig. 3C-D, Suppl. Table 7A). No overlap of DEGs has been observed in SAT between men and women. In SAT of men, Reactome enrichment is significant for estrogen receptor mediated signaling (*MMP9, FKBP5*; without FDR-adjustment) and tumor necrosis factor (TNF) superfamily (*COLEC12, ENAH, TNFRSF12A, DLC1, PTX3, MMP9*; Suppl. Table 7B). IPA enrichment for diseases and biological function highlights immune response pathways (*MMP9*) similar to SAT in women (Suppl. Table 7C). The inclusion of clinical parameters uncovered a significant correlation between fT4 levels and ETD accumulation, which is further substantiated by correlation of corresponding DEGs (Fig. 4). *MMP9* is associated with fasting plasma glucose concentrations (Fig. 4, Suppl. Table 7D). Furthermore, *PTX3, MMP9, ADAMTS5, FOSL1* and *TNFRSF12A* are clustering together at the protein level according to the StringDB network analysis (Suppl. Figure 6) giving further confidence that above shown enrichment effects are not driven by outliers.

We repeated the gene expression analysis in VAT. The list of DEG in VAT from women includes *COL1A1, TNFRSF11A, CD83* and *ITGAM* (Fig. 3E-F, Suppl. Table 8A). Enrichment with IPA yields several associations with immune response (e.g. binding of dendritic cells), connective tissue disorder (e.g. inflammation of joint), Hashimoto thyroiditis (*CD83*) and cardiovascular function (e.g. adhesion of microvascular endothelial cells). Further analysis with StringDB supports predicted interactions between translation products of DEGs including *ITGAM* and *THY1* which are associated with a STRING cluster for GPI anchor binding (Suppl. Figure 7). In VAT from men, only three control samples without ETD accumulation signal were available. DEGs include *LEP,* DDR*2, ESYT2* and multiple human leukocyte antigens *(*HLA*)* and are enriched for inflammatory response (e.g. Degranulation of CD8+ *T* lymphocyte) and adipose tissue and reproductive function (*LEP*) according to the IPA disease and biological function database (Suppl. Tables 9A, 9C). StringDB network analysis highlights functional connection of HLA genes (Suppl. Figure 8). In women's VAT, the DEG expression signal showed a partial correlation with fT3, although this association was not mirrored by the ETD accumulation signal (Fig. 4). In contrast, analysis of VAT from men revealed a link between ETD accumulation and total cholesterol, which was partially validated by corresponding DEGs (Fig. 4, Suppl. Tables 8D, 9D).

Upstream regulator enrichment analysis highlights associations with inflammatory pathways

The previous analysis reveals that the overall DEG profiles and their associations with POP accumulation are highly heterogeneous, varying significantly across sex, fat depot, and distinct POP accumulation groups. As summarized in Fig. 5A, the top enriched disease annotations identified by IPA (without p-value adjustment for multiple testing) differ substantially between subgroups. Notably, individual DEGs are annotated to a diverse array of pathways, with minimal overlap between conditions. Despite this complexity, the pathways are predominantly characterized by inflammatory responses, including cell migration, T lymphocyte proliferation, Th1 cell cytotoxicity, and leukocyte activation. To provide further context for the identified DEGs, we conducted an upstream regulator analysis using IPA (Fig. 5B) which predicts regulators that are likely to be responsible for the observed gene expression changes. This analysis revealed a common set of top upstream regulators across different subgroups, suggesting that the identified DEGs are regulated by similar molecular mechanisms. Notably, the top regulatory genes include various interleukins (e.g., CXCL8, IL1B, IL3, IL4, IL13), TNF, and interferon gamma (IFNG), all of which are associated with inflammatory functions. This finding supports our observation that, despite the lacking overlap in individual DEGs, the overall effects are linked to inflammation and immune responses, highlighting a shared underlying biology.

Toxicity list enrichment reveals trends for retinoid acid receptor activity

In addition, we considered toxicity lists in the IPA database to link the experimental DEGs to potential pathological endpoints. The results show various associations with DEGs from different groups as depicted in Fig. 5C. Significant effects (without p-value adjustment) include liver

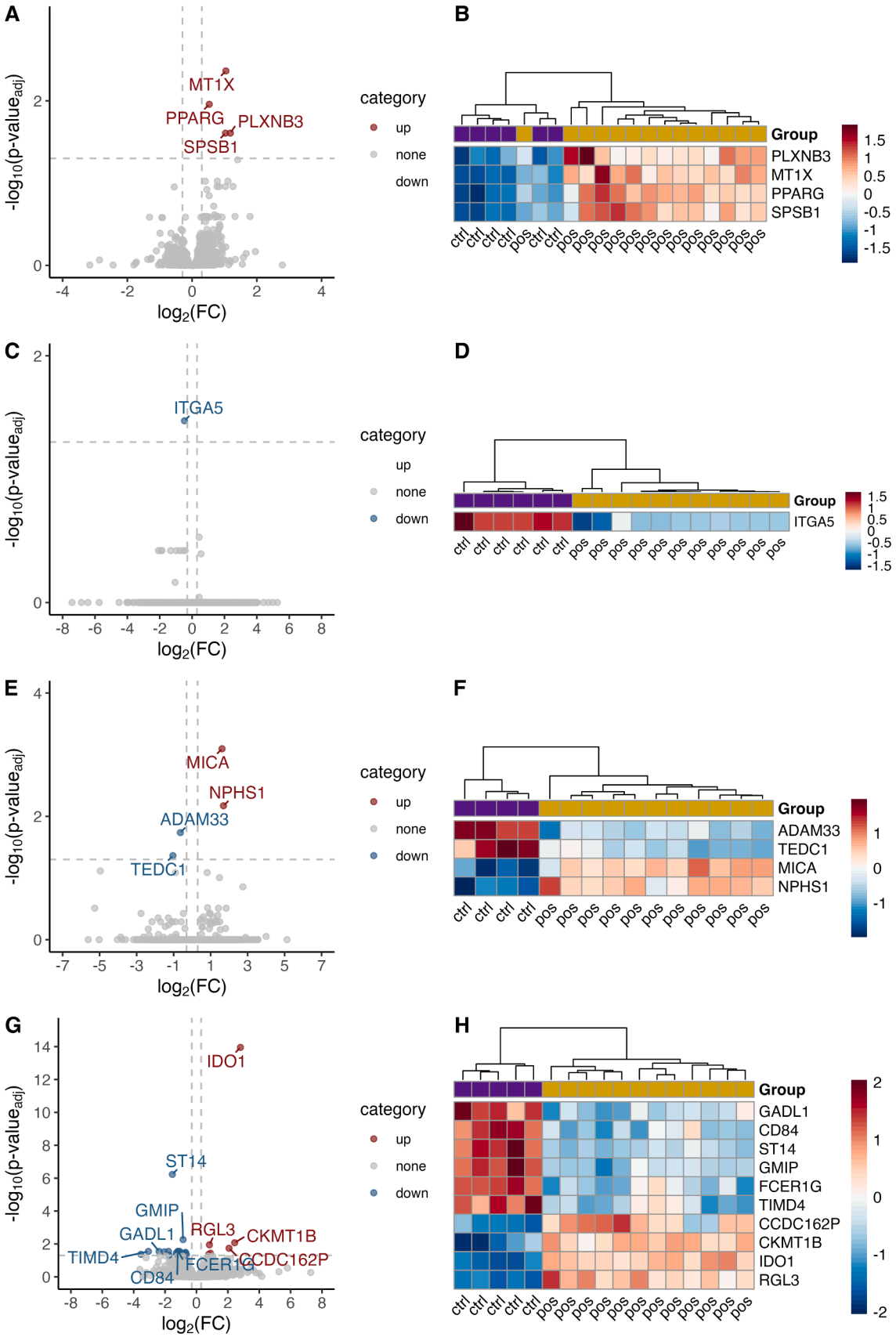

Fig. 1. Differentially expressed genes (DEGs) for the contrast of DIPB positive individuals and controls in SAT of A-B) women and C-D) men and VAT of E-F) women. G-H) highlight the top ten DEGs of VAT in men. Complete lists of DEGs are reported in suppl. tables 2A, 3A, 4A and 5A respectively.

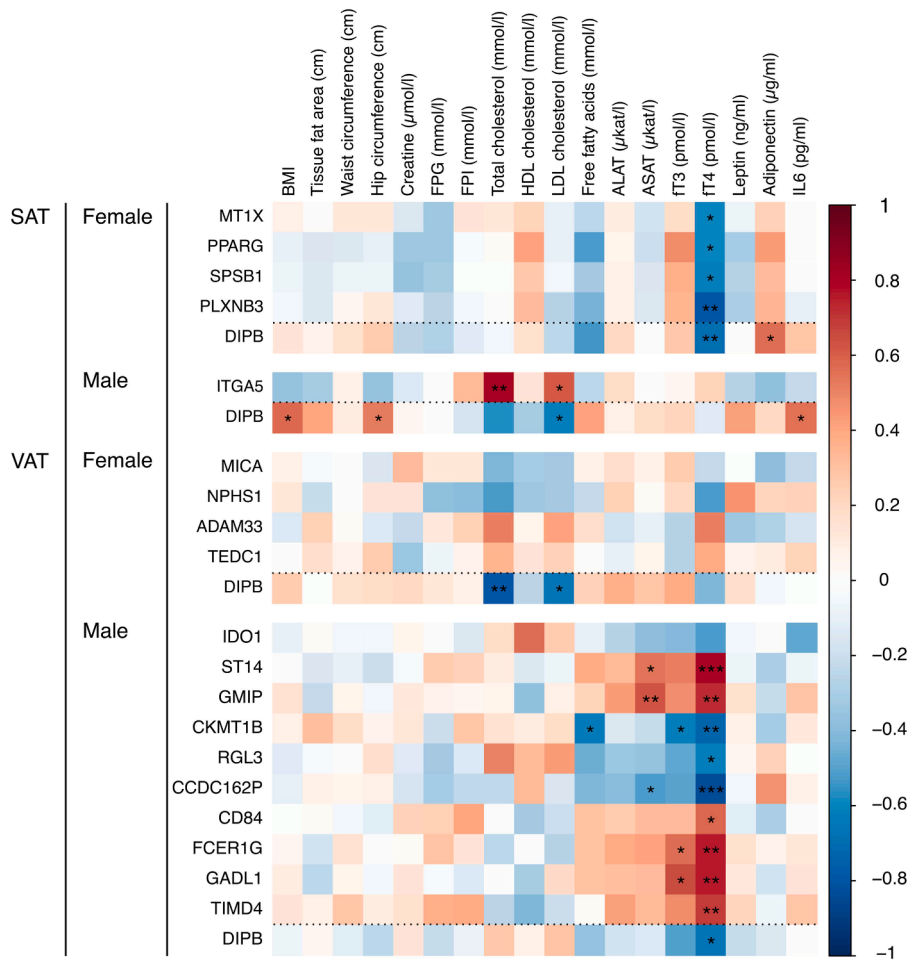

Fig. 2. Spearman's correlation analysis results of DIPB accumulation signals and the normalized expression values of the top ten differentially expressed genes (ranked by fold change) in relation to DIBP groups to assess associations with clinical parameters. Analysis was conducted separately for SAT and VAT in both men and women. P-values are not adjusted for multiple testing and indicated as * <0.05, ** < 0.01, *** < 0.001. Raw correlation values are reported in suppl. tables 2D, 3D, 4D and 5D for each condition respectively.

stenosis and stress response particular under ETD exposure in men and NF-κB signaling in AT from women under ETD exposure and VAT from men under DIPB exposure. Interestingly, many genes across groups show activation of retinoid acid receptor (RAR), retinoic X receptor (RXR) and various heterodimers of RXR. Despite not being significant in all tested conditions, the prevalence of these associations in view of the variability of detected DEGs is particularly striking.

Discussion

In our exploratory studies, aimed to gaining insights into the molecular mechanisms underlying the effects of POPs on human health, we investigated the relationship between AT accumulation of DIPB and ETD and gene expression signatures in visceral and abdominal subcutaneous fat. Our study design included a diverse cohort of human donors, allowing us to explore the interplay between POP exposure, gene expression, and various anthropometric and glucose metabolism parameters. Our previous data on human AT POP accumulation (Rolle-Kampczyk et al., 2020) was reexamined in conjunction with newly performed RNA-Seq global gene expression data. We performed a stringent comparative analysis of gene expression patterns between individuals with and without accumulated POPs in both SAT and VAT depots. The main objective was to identify specific genes and pathways that may underly the proposed link between high DIPB and ETD abundance in AT with altered AT function parameters and the phenotype of AT donors.

In general, differentially gene expression analysis between individuals with positive DIPB or ETD abundance and controls identified several genes that do not overlap in men and women or fat depots, suggesting individual effects specific for sex, POP and AT depot. Nevertheless, we observed coherent associations between AT gene expression signatures, DIPB and/or ETD abundance and parameters of AT function and human phenotypes that we discuss in more detail. Previous adjustment of the gene expression data for BMI and age removes the potential confounding influences of obesity and aging processes. POPs are known to accumulate in adipose tissue at low concentrations and are believed to induce subtle changes in gene expression rather than strong transcriptional responses (La Merrill et al., 2013). Unlike conditions such as severe diseases or inflammatory states, where large numbers of DEGs are typically observed, the expected effects of POP exposure are modest. The small number of FDR-corrected DEGs we identified likely reflects these subtle biological effects rather than limitations in statistical power alone. Furthermore, the clear separation between control and POP exposure groups within the first two principal components provides a solid foundation for identifying a small yet statistically relevant set of genetic drivers. Given the exploratory nature of our study, applying FDR correction across all genes would have resulted in too few candidates for meaningful pathway analysis. Therefore, we employed a less stringent threshold (without FDR correction) to select genes for enrichment analysis. This approach is common in exploratory studies aimed at generating hypotheses about biological pathways rather than drawing definitive mechanistic conclusions (Bender and

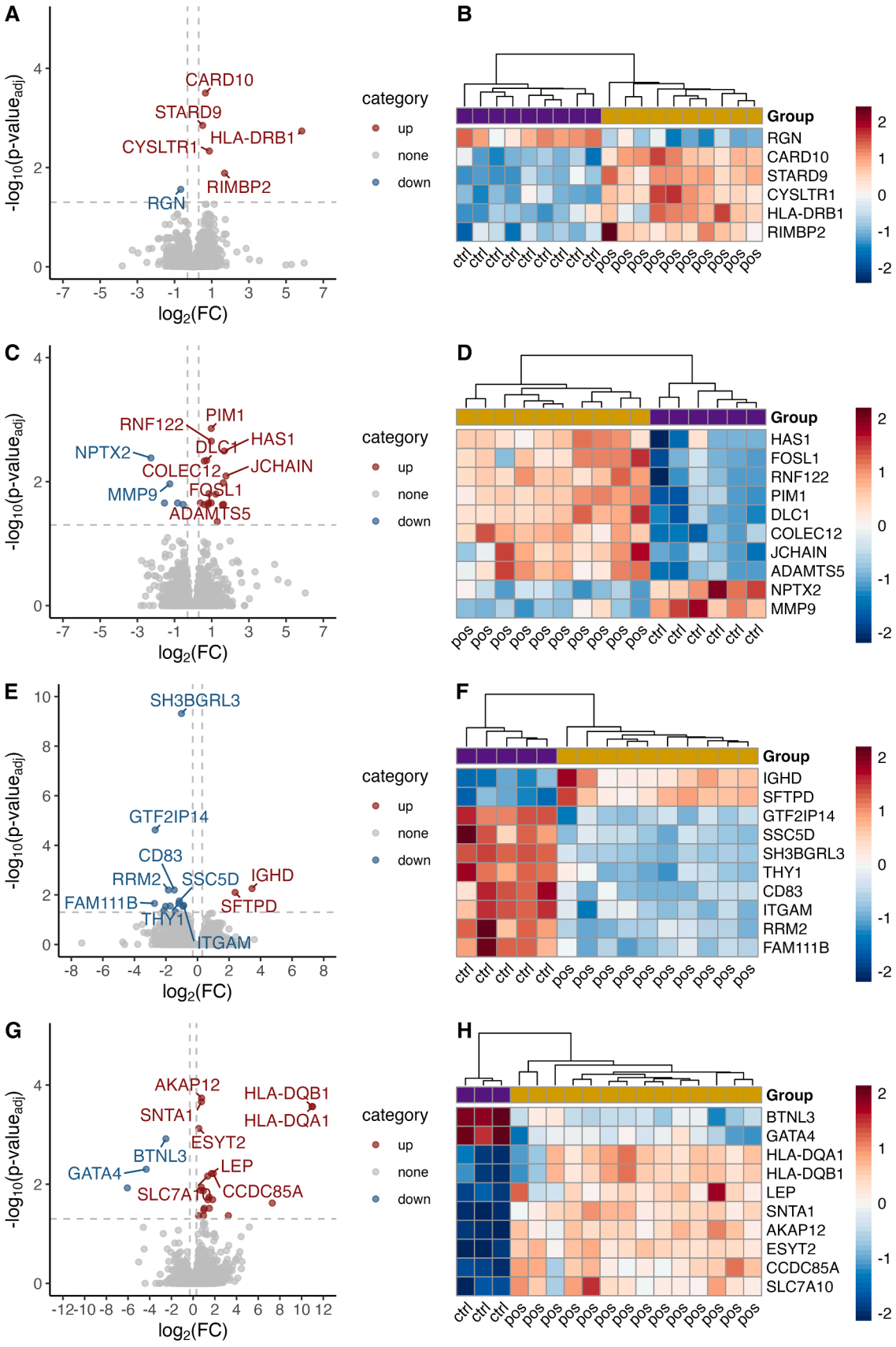

Fig. 3. Differentially expressed genes (DEGs) for the contrast of ETD positive individuals and controls in SAT of A-B) women and C-D) men and VAT of E-F) women and G-H) men. For C—H, the top ten DEGs are shown. Complete lists of DEGs are reported in suppl. tables 6A, 7A, 8A and 9A respectively.

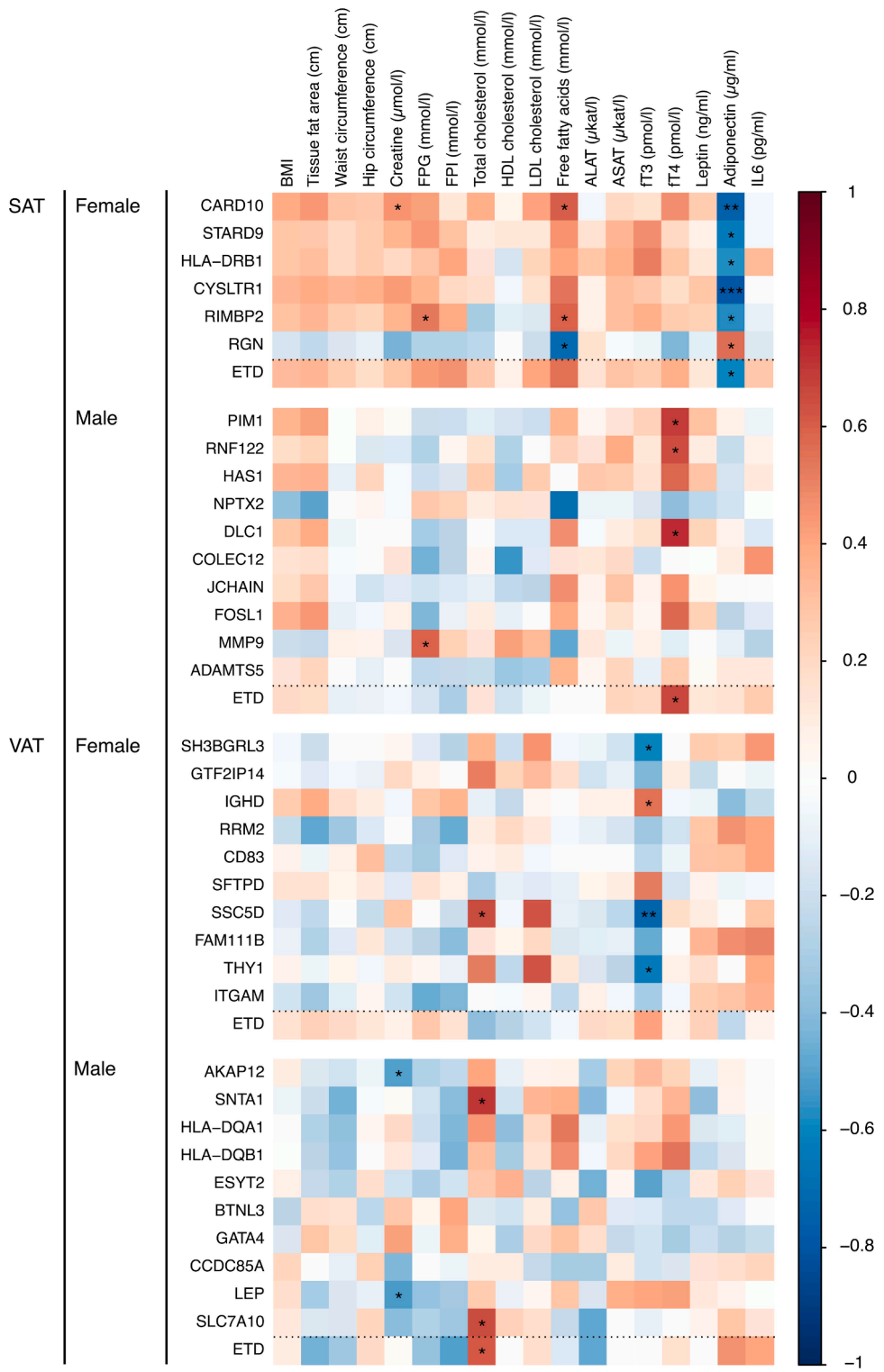

Fig. 4. Spearman's correlation analysis results of ETD accumulation signals and the normalized expression values of the top ten differentially expressed genes (ranked by fold change) in relation to ETD groups to assess associations with clinical parameters. Analysis was conducted separately for SAT and VAT in both men and women. P-values are not adjusted for multiple testing and indicated as * <0.05, ** < 0.01, *** < 0.001. Raw correlation values for all genes are reported in suppl. tables 6D, 7D, 8D and 9D for each condition respectively.

Lange, 2001). Consequently, this exploratory strategy is particularly appropriate when investigating modest effects, as strict correction methods might eliminate potentially relevant candidates.

DIPB and/or ETD abundance is associated with gene signatures of immune response, NF-κB signaling and PPARγ

Enrichment analysis of DEGs shows prevalent association with pathways related to immune response in both male and female SAT and VAT in relation to DIPB and ETD abundance. More specifically, nuclear

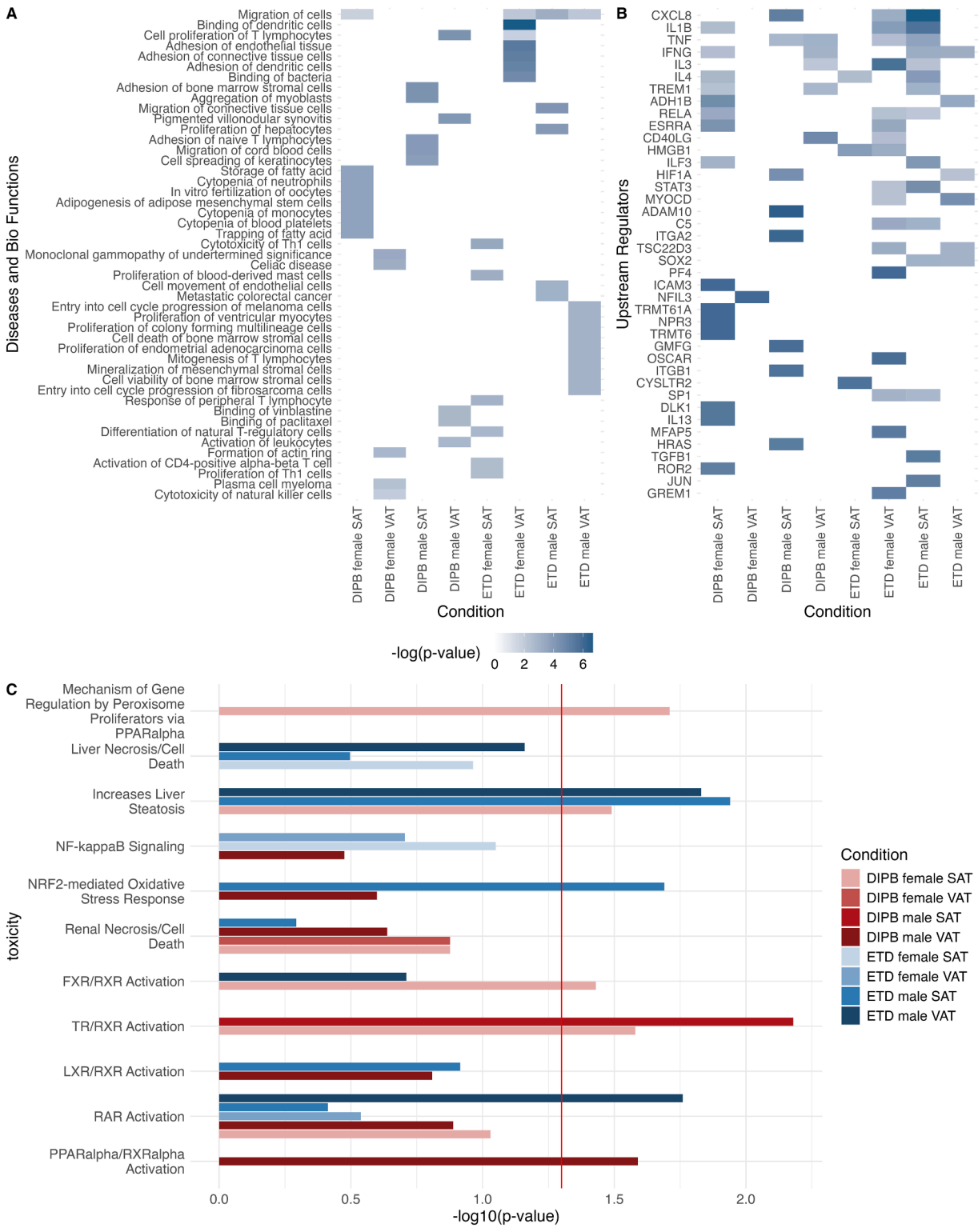

Fig. 5. Heatmap of IPA results showing (A) the top five enriched disease associations and (B) the top 40 significant upstream regulator genes across all analyzed groups. Raw data are reported in Suppl. Table 10. C) Enrichment of selected toxicity endpoints with IPA. The red line indicates the significance level of $p = 0.05$. All shown p-values are not adjusted for multiple testing.

factor-κB (NF-κB) signaling is enriched in VAT of men with high DIPB AT concentrations and female SAT and VAT under high ETD abundance. AT inflammation is an important symptom of AT dysfunction in obesity (Blüher, 2013). The transition of normal AT function to AT inflammation is partly driven by cellular stress induced activation of NF-κB pathways among others (Shoelson et al., 2006; Blüher, 2016). More specific, two genes in our analysis are highlighted with NF-κB signaling enrichment and linked to obesity and inflammation in the literature: *FCER1G* (Fc fragment of IgE receptor; differentially regulated under DIPB accumulation in VAT of men) where it has been shown that *FCER1G* deficiency in Fc-receptor-γ-chain knock-out mice develop diet-induced obesity, white AT inflammation and insulin resistance (Van

Beek et al., 2015); and *CARD10* (regulated under ETD accumulation in SAT of women), which was reported as being suppressed by induced inflammation and obesity in human *in-vivo* experiments (Shah et al., 2012).

Additionally, we identified *PPARG* as major candidate gene for the association between POP accumulation and AT dysfunction in SAT of women. Given the pivotal role of peroxisome proliferator-activated receptor gamma (PPARγ) as a master regulator of adipogenesis and adipocyte differentiation (Tontonoz and Spiegelman, 2008), our findings imply that variations in POP accumulation in AT may play a contributing role in the development of increased AT mass and AT dysfunction, which are hallmarks of obesity. Supporting this notion, lower serum POP concentrations have been found in individuals with metabolically healthy obesity – a condition that is related to preserved normal AT function and low levels of inflammatory parameters despite high fat mass (Blüher, 2020; Gauthier et al., 2014). Furthermore, we previously found significant associations between macrophage infiltration into AT and ETD and DIPB accumulation particularly in lean women (Rolle-Kampczyk et al., 2020). The detection of NF-κB pathway activation and PPARγ signaling in specific AT depots as strongly associated with ETD and DIPB abundance extends previous findings (Rolle-Kampczyk et al., 2020) suggesting that stress-induced inflammatory AT dysfunction could be related to DIPB and ETD. Whether associations of NF-κB signaling and POP concentrations are specifically regulated in women by DIPB and in men by ETD needs to be validated in future exposure studies.

DIPB and ETD abundance is associated with retinoic acid receptor activation

In the IPA enrichment analysis, we identified retinoic acid (RA) receptor and retinoid X receptor (RXR) activation as strongly associated with DIPB and ETD bioaccumulation in AT Despite not being significant under all test conditions, this effect is seen throughout all groups under high DIPB and ETD AT abundance. RA is a bioactive metabolite derived from Vitamin A activating retinoid receptors, which can heterodimerize with PPAR and T3 receptors (Villarroya et al., 1999). The activation of RA receptors is known to promote adipose tissue browning via upregulation of uncoupling protein-1 (UCP-1) (Alvarez et al., 1995). The browning of white adipose tissue induced by RA has been experimentally shown in mice (Mercader et al., 2006; Wang et al., 2017). A recent study reported that knockout of RARα in mice revealed increased risk for obesity and steatohepatitis independent of diet, reduced thermogenesis, and increased inflammatory effects in AT, suggesting that RARα prevents obesity and inflammatory AT dysfunction (Cassim Bawa et al., 2024). Our finding of systematic trends in RAR and RXR activation in relation to higher AT POP concentrations may suggest that these POPs could influence AT browning via RA receptor activation and thereby contribute to phenotype differences between people with high versus low DIPB and ETD exposure. In 236 individuals of the GraMo adult cohort, retinoid system markers have been analyzed under influence of PCBs revealing increasing levels of PCBs with decreased retinol levels in AT and increasing retinol binding protein 4 to retinol ratio in serum which further suggests a link between the retinoid system and levels of POP in AT (Galbán-Velázquez et al., 2021). In our analysis, one example of a gene enriched for RAR activation (in ETD accumulation among men) is the matrix metalloproteinase *MMP9*. Matrix metalloproteinases mediate extracellular matrix remodeling which takes place during obesity-induced AT formation as shown in differential gene expression analysis of white AT in rats (Chavey et al., 2003). Studies have linked *MMP9* expression in humans to insulin resistance and obesity (Ritter et al., 2017; Unal et al., 2010). In our data, differential *MMP9* expression signal is enriched for the toxicologic endpoint of RAR activation and correlates directly with fasting plasma glucose concentrations. Under the assumptions, that firstly RAR activation mediates AT browning therefore regulating energy expenditure and thermogenesis (Cassim Bawa et al., 2024), and that secondly thermogenesis is linked to glucose homeostasis (Keinan et al., 2021), the finding that *MMP9* correlates with plasma glucose levels is plausible.

POPs may have effects on thyroid hormones and adipokines

Differentially expressed genes in AT between DIPB positive individuals and controls correlate with fT4 in SAT from women and in VAT from men. In contrast, the comparison between ETD positive individuals and controls highlights individual DEGs correlating with fT4 (SAT in men) and fT3 (SAT in women). This suggests a link between DIPB and ETD with thyroid homeostasis that is reflected by distinct gene expression signatures in AT depots, depending on sex and DIPB or ETD. It remains unclear whether POPs may directly affect thyroid and AT function in parallel or whether alterations in AT function upon POP exposure may change signals altering thyroid hormone levels. Recent investigations have shed light on the relationship between POPs and thyroid hormones, revealing significant associations between POP exposure and thyroid diseases in various populations. Specifically, studies in Asian populations have linked polychlorinated biphenyls (PCBs), polybrominated diphenyl ethers (PBDEs), and organochlorine pesticides (OCPs) to thyroid disease (Kim et al., 2013; Han et al., 2019). Similarly, a study in French children found associations between thyroid disease and exposure to PCBs, OCPs, and per- and polyfluoroalkyl substances (PFASs) (Tillaut et al., 2022). Although substances analyzed in the above-mentioned case-control studies differ from pollutants investigated in our study, the independently observed associations indicate that POPs may play a role in regulation of thyroid function. Together with data from other groups, our data suggest that thyroid hormone alterations could be induced through a variety of chemical classes of POPs. Moreover, detected associations of DIPB include thyroid receptor (TR)/RXR activation. In that regard, it is plausible that influence of POPs on the activation of TR/RXR heterodimers also influences thyroid hormone levels. However, our data cannot answer the question how TR/RXR activation, POP exposure and serum thyroid levels are mechanistically connected. However, our data may stimulate future studies investigating the role of DIPB and ETD on thyroid hormones.

Supporting the hypothesis that abundance of POPs in AT may contribute to AT dysfunction, we find that adiponectin is correlating with ETD accumulation associated DEGs in SAT of women. Adiponectin is a highly abundant adipokine that is associated with central body fat distribution, insulin sensitivity and associated in high serum concentrations with a healthier phenotype (Staiger et al., 2003; Cnop et al., 2003).

We reported sex-specific associations of waist-hip-ratio with DIPB signal in VAT and ETD signal in SAT in women (Rolle-Kampczyk et al., 2020). Our finding that adiponectin regulation in women is related to high ETD concentrations in AT is consistent with results from the previous study emphasizing potential contribution of POPs to sex-specific alteration of fat distribution. In fact, many POPs are known to be endocrine disrupting (Bonefeld-Jørgensen et al., 2001), acting sex-specific and potentially affect female reproduction (Gregoraszczuk and Ptak, 2013).

Limitations

Despite seeing comprehensive effects across different tested groups, the small sample size and the typical human heterogeneity within the cohort are both limitations to the strength and specificity of detected effects. Additionally, the modest biological effects of POP exposure and the exploratory nature of our analysis (employing less stringent thresholds without FDR correction) limit the ability to draw definitive mechanistic conclusions. Therefore, generalizability of the results is limited and to draw definitive mechanistic conclusions of AT response to POP exposure is beyond the scope of this study. While we cannot comment on whether the genes listed in this study are indeed regulated

specific to sex groups, AT depots or POP exposures, we are able to determine consistent regulatory effects in line with the literature throughout the different groups which gives confidence in the robustness of our analysis and the capability to detect main drivers in the gene expression response to POP exposure. In summary, we are able to gain initial insights into genome-wide inflammatory and functional effects that POP accumulation might have on adipose tissue. However, these findings are exploratory in nature and require validation through larger follow-up studies or targeted functional studies. The causal relationships between gene expression changes and phenotypic outcomes such as fat browning or inflammation levels have not yet been experimentally validated. Future research involving mechanistic experiments will be necessary to confirm these associations.

Conclusion

In conclusion, our study demonstrates that the accumulation of DIPB and ETD in adipose tissue is linked to alterations in AT function and inflammation, with sex- and depot-specific gene expression profiles revealing associations with immune responses, NF-κB signaling, and PPARγ pathways. Furthermore, our results suggest that POP exposure may influence AT browning through altered retinoid acid receptor activity. Notably, our findings highlight specific genes that may be directly regulated by high abundance of DIPB and ETD, including adiponectin, leptin, PPARγ, interleukins, NF-κB, which are resembling disease mechanisms of obesity. Future studies are necessary to elucidate the precise mechanisms by which DIPB, ETD or other POPs induce AT dysfunction. Moreover, our work highlights the need for larger cohort studies that incorporate functional experiments and multi-omics approaches. The utilization of single-nuclei sequencing techniques in future research could provide insights into cell type-specific responses, allowing for a more detailed examination of the genetic mechanisms underlying the influence of POPs on adipose tissue dysfunction and to explore the potential links between POP exposure and metabolic disorders. Ultimately, this research underscores the importance of considering the role of environmental pollutants in the development of metabolic disorders.

Informed consent statement

The study was approved by the Ethics Committee of the University of Leipzig (approval no: 159-12-21052012) and was performed in accordance with the Declaration of Helsinki. All study participants gave written informed consent before taking part in the study.

CRediT authorship contribution statement

Tobias Hagemann: Writing – review & editing, Writing – original draft, Visualization, Methodology, Formal analysis. **Ulrike Rolle-Kampczyk:** Writing – review & editing, Formal analysis. **Kristin Schubert:** Writing – review & editing. **Arne Dietrich:** Writing – original draft. **Martin von Bergen:** Writing – review & editing, Funding acquisition, Data curation, Conceptualization. **Matthias Blüher:** Writing – review & editing, Funding acquisition, Data curation, Conceptualization. **Anne Hoffmann:** Writing – review & editing, Supervision, Methodology, Conceptualization.

Declaration of competing interest

MB received honoraria as a consultant and speaker from Amgen, AstraZeneca, Bayer, Boehringer-Ingelheim, Lilly, Novo Nordisk, Novartis, and Sanofi. All other authors declare no conflicts of interest. The funders had no role in the design of the study; in the collection, analyses, or interpretation of data; in the writing of the manuscript; or in the decision to publish the results.

Funding

MB received funding from grants from the Deutsche Forschungsgemeinschaft (DFG, German Research Foundation), project number 209933838 – SFB 1052 (project B1) and by German Centre for Diabetes Research (DZD, Deutsches Zentrum für Diabetesforschung), grant 82DZD00601. MvB received funding from grants from the DFG project number 209933838 – SFB 1052 (project B1 and Z3). KS is grateful for funding from the DFG, project number 530364326.

Acknowledgements

We thank all patients and their families for participating in this study.

Supplementary materials

Supplementary material associated with this article can be found, in the online version, at doi:10.1016/j.envadv.2025.100655.

Data availability

The raw RNA-Seq data are publicly available in the Sequence Read Archive (SRA) under BioProject ID PRJNA1284331.

References

Alvarez, R., De Andrés, J., Yubero, P., Viñas, O., Mampel, T., Iglesias, R., et al., 1995. A novel regulatory pathway of brown fat thermogenesis. J. Biol. Chem. 270 (10), 5666–5673. https://doi.org/10.1074/jbc.270.10.5666.

Barouki, R., 2010. Linking long-term toxicity of xeno-chemicals with short-term biological adaptation. Biochimie 92 (9), 1222–1226. https://doi.org/10.1016/j.biochi.2010.02.026.

Bender, R., Lange, S., 2001. Adjusting for multiple testing—when and how? J. Clin. Epidemiol. 54 (4), 343–349. https://doi.org/10.1016/S0895-4356(00)00314-0.

Blüher, M., 2009. Adipose tissue dysfunction in obesity. Exp. Clin. Endocrinol. Diabetes 117 (6), 241–250. https://doi.org/10.1055/s-0029-1192044.

Blüher, M., 2013. Adipose tissue dysfunction contributes to obesity related metabolic diseases. Best Pract. Res. Clin. Endocrinol. Metab. 27 (2), 163–177. https://doi.org/10.1016/j.beem.2013.02.005.

Blüher, M., 2016. Adipose tissue inflammation: a cause or consequence of obesity-related insulin resistance? Clin. Sci. (Lond. Engl.: 1979) 130 (18), 1603–1614. https://doi.org/10.1042/CS20160005.

Blüher, M., 2020. Metabolically healthy obesity. Endocr. Rev. 41 (3), bnaa004. https://doi.org/10.1210/endrev/bnaa004.

Bonefeld-Jørgensen, E.C., Andersen, H.R., Rasmussen, T.H., Vinggaard, A.M., 2001. Effect of highly bioaccumulated polychlorinated biphenyl congeners on estrogen and androgen receptor activity. Toxicology 158 (3), 141–153. https://doi.org/10.1016/S0300-483X(00)00368-1.

Cassim Bawa, F.N., Hu, S., Gopoju, R., Shiyab, A., Mongan, K., Xu, Y., et al., 2024. Adipocyte retinoic acid receptor α prevents obesity and steatohepatitis by regulating energy expenditure and lipogenesis. Obesity 32 (1), 120–130. https://doi.org/10.1002/oby.23929.

Chavey, C., Mari, B., Monthouel, M.-N., Bonnafous, S., Anglard, P., Van Obberghen, E., et al., 2003. Matrix metalloproteinases are differentially expressed in adipose tissue during obesity and modulate adipocyte differentiation. J. Biol. Chem. 278 (14), 11888–11896. https://doi.org/10.1074/jbc.M209196200.

Chen, E.Y., Tan, C.M., Kou, Y., Duan, Q., Wang, Z., Meirelles, G.V., et al., 2013. Enrichr: interactive and collaborative HTML5 gene list enrichment analysis tool. BMC Bioinform. 14 (1), 128. https://doi.org/10.1186/1471-2105-14-128.

Cnop, M., Havel, P.J., Utzschneider, K.M., Carr, D.B., Sinha, M.K., Boyko, E.J., et al., 2003. Relationship of adiponectin to body fat distribution, insulin sensitivity and plasma lipoproteins: evidence for independent roles of age and sex. Diabetologia 46 (4), 459–469. https://doi.org/10.1007/s00125-003-1074-z.

Croft, D., O'Kelly, G., Wu, G., Haw, R., Gillespie, M., Matthews, L., et al., 2011. Reactome: a database of reactions, pathways and biological processes. Nucleic Acids Res. 39 (1), D691–D697. https://doi.org/10.1093/nar/gkq1018.

Crowson, C.S., Matteson, E.L., Davis, J.M., Gabriel, S.E., 2013. Contribution of obesity to the rise in incidence of rheumatoid arthritis. Arthritis Care Res. 65 (1), 71–77. https://doi.org/10.1002/acr.21660.

Dobin, A., Davis, C.A., Schlesinger, F., Drenkow, J., Zaleski, C., Jha, S., et al., 2013. STAR: ultrafast universal RNA-seq aligner. Bioinformatics 29 (1), 15–21. https://doi.org/10.1093/bioinformatics/bts635.

Fasshauer, M., Blüher, M., 2015. Adipokines in health and disease. Trends Pharmacol. Sci. 36 (7), 461–470. https://doi.org/10.1016/j.tips.2015.04.014.

Fisher, B.E., 1999. Most unwanted. Environ. Health Perspect. 107 (1), A18–A23.

Flores-Cordero, J.A., Pérez-Pérez, A., Jiménez-Cortegana, C., Alba, G., Flores-Barragán, A., Sánchez-Margalet, V., 2022. Obesity as a risk factor for dementia and

Alzheimer's Disease: the role of leptin. Int. J. Mol. Sci. 23 (9), 5202. https://doi.org/10.3390/ijms23095202.
Galbán-Velázquez, S., Esteban, J., Çakmak, G., Artacho-Cordón, F., León, J., Barril, J., et al., 2021. Associations of persistent organic pollutants in human adipose tissue with retinoid levels and their relevance to the redox microenvironment. Environ. Res. 195, 110764. https://doi.org/10.1016/j.envres.2021.110764.
Gauthier, M.-S., Rabasa-Lhoret, R., Prud'homme, D., Karelis, A.D., Geng, D., van Bavel, B., et al., 2014. The metabolically healthy but obese phenotype is associated with lower plasma levels of persistent organic pollutants as compared to the metabolically abnormal obese phenotype. J. Clin. Endocrinol. Metab. 99 (6), E1061–E1066. https://doi.org/10.1210/jc.2013-3935.
Gregoraszczuk, E.L., Ptak, A., 2013. Endocrine-disrupting chemicals: some actions of POPs on female reproduction. Int. J. Endocrinol. 2013 (1), 828532. https://doi.org/10.1155/2013/828532.
Han, X., Meng, L., Li, Y., Li, A., Turyk, M.E., Yang, R., et al., 2019. Associations between exposure to persistent organic pollutants and thyroid function in a case-control study of East China. Environ. Sci. Technol. 53 (16), 9866–9875. https://doi.org/10.1021/acs.est.9b02810.
Imai, K., Keele, L., Tingley, D., 2010. A general approach to causal mediation analysis. Psychol. Methods 15 (4), 309–334. https://doi.org/10.1037/a0020761.
Jawaid, W., 2023. EnrichR: provides an R interface to "Enrichr".
Kanehisa, M., Sato, Y., Kawashima, M., Furumichi, M., Tanabe, M., 2016. KEGG as a reference resource for gene and protein annotation. Nucleic Acids Res. 44 (D1), D457–D462. https://doi.org/10.1093/nar/gkv1070.
Keinan, O., Valentine, J.M., Xiao, H., Mahata, S.K., Reilly, S.M., Abu-Odeh, M., et al., 2021. Glycogen metabolism links glucose homeostasis to thermogenesis in adipocytes. Nature 599 (7884), 296–301. https://doi.org/10.1038/s41586-021-04019-8.
Kershaw, E.E., Flier, J.S., 2004. Adipose tissue as an endocrine organ. J. Clin. Endocrinol. Metab. 89 (6), 2548–2556. https://doi.org/10.1210/jc.2004-0395.
Kim, S., Park, J., Kim, H.-J., Lee, J.J., Choi, G., Choi, S., et al., 2013. Association between several persistent organic pollutants and thyroid hormone levels in serum among the pregnant women of Korea. Environ. Int. 59, 442–448. https://doi.org/10.1016/j.envint.2013.07.009.
Klöting, N., Fasshauer, M., Dietrich, A., Kovacs, P., Schön, M.R., Kern, M., et al., 2010. Insulin-sensitive obesity. Am. J. Physiol.-Endocrinol. Metab. 299 (3), E506–E515. https://doi.org/10.1152/ajpendo.00586.2009.
Krämer, A., Green, J., Pollard, J., Tugendreich, S., 2014. Causal analysis approaches in ingenuity pathway analysis. Bioinformatics 30 (4), 523–530. https://doi.org/10.1093/bioinformatics/btt703.
La Merrill, M., Emond, C., Kim, M.J., Antignac, J.P., Le Bizec, B., Clément, K., et al., 2013. Toxicological function of adipose tissue: focus on persistent organic pollutants. Environ. Health Perspect. 121 (2), 162–169. https://doi.org/10.1289/ehp.1205485.
Langhardt, J., Flehmig, G., Klöting, N., Lehmann, S., Ebert, T., Kern, M., et al., 2018. Effects of weight loss on glutathione peroxidase 3 serum concentrations and adipose tissue expression in Human obesity. Obes. Facts 11 (6), 475–490. https://doi.org/10.1159/000494295.
Lee, D.-H., Porta, M., Jacobs, D.R., Vandenberg, L.N., 2014. Chlorinated persistent organic pollutants, obesity, and type 2 diabetes. Endocr. Rev. 35 (4), 557–601. https://doi.org/10.1210/er.2013-1084.
Leek, J.T., Johnson, W.E., Parker, H.S., Fertig, E.J., Jaffe, A.E., Storey, J.D., et al., 2019. Sva: surrogate variable analysis. R Package Ver. 3 (0), 882–883.
Leek, J.T., 2014. Svaseq: removing batch effects and other unwanted noise from sequencing data. Nucleic Acids Res. 42 (21), e161. https://doi.org/10.1093/nar/gku864.
Lehr, S., Hartwig, S., Sell, H., 2012. Adipokines: a treasure trove for the discovery of biomarkers for metabolic disorders. PROTEOM. – Clin. Appl. 6 (1–2), 91–101. https://doi.org/10.1002/prca.201100052.
Liao, Y., Smyth, G.K., Shi, W., 2014. FeatureCounts: an efficient general purpose program for assigning sequence reads to genomic features. Bioinformatics 30 (7), 923–930. https://doi.org/10.1093/bioinformatics/btt656.
Mercader, J., Ribot, J., Murano, I., Felipe, F., Cinti, S., Bonet, M.L., et al., 2006. Remodeling of white adipose tissue after retinoic acid administration in mice. Endocrinology 147 (11), 5325–5332. https://doi.org/10.1210/en.2006-0760.
Michael Love, S.A., 2017. DESeq2. Bioconductor.
Mokdad, A.H., Ford, E.S., Bowman, B.A., Dietz, W.H., Vinicor, F., Bales, V.S., et al., 2003. Prevalence of obesity, diabetes, and obesity-related health risk factors, 2001. JAMA 289 (1), 76–79. https://doi.org/10.1001/jama.289.1.76.
N.d. Babraham bioinformatics - FastQC a quality control tool for high throughput sequence data. https://www.bioinformatics.babraham.ac.uk/projects/fastqc/. [accessed July 5, 2024].
Ortega, F.B., Lavie, C.J., Blair, S.N., 2016. Obesity and cardiovascular disease. Circ. Res. 118 (11), 1752–1770. https://doi.org/10.1161/CIRCRESAHA.115.306883.
Ritchie, M.E., Phipson, B., Wu, D., Hu, Y., Law, C.W., Shi, W., et al., 2015. Limma powers differential expression analyses for RNA-sequencing and microarray studies. Nucleic Acids Res. 43 (7), e47. https://doi.org/10.1093/nar/gkv007.
Ritter, A.M.V., de Faria, A.P., Barbaro, N., Sabbatini, A.R., Corrêa, N.B., Brunelli, V., et al., 2017. Crosstalk between obesity and MMP-9 in cardiac remodelling –a cross-sectional study in apparent treatment-resistant hypertension. Blood Press. 26 (2), 122–129. https://doi.org/10.1080/08037051.2016.1249336.
Rodríguez-Hernández, H., Simental-Mendía, L.E., Rodríguez-Ramírez, G., Reyes-Romero, M.A., 2013. Obesity and inflammation: epidemiology, risk factors, and markers of inflammation. Int. J. Endocrinol. 2013 (1), 678159. https://doi.org/10.1155/2013/678159.
Rohm, T.V., Meier, D.T., Olefsky, J.M., Donath, M.Y., 2022. Inflammation in obesity, diabetes, and related disorders. Immunity 55 (1), 31–55. https://doi.org/10.1016/j.immuni.2021.12.013.
Rolle-Kampczyk, U., Gebauer, S., Haange, S.-B., Schubert, K., Kern, M., Moulla, Y., et al., 2020. Accumulation of distinct persistent organic pollutants is associated with adipose tissue inflammation. Sci. Total Environ. 748, 142458. https://doi.org/10.1016/j.scitotenv.2020.142458.
Schneider, V.A., Graves-Lindsay, T., Howe, K., Bouk, N., Chen, H.-C., Kitts, P.A., et al., 2017. Evaluation of GRCh38 and de novo haploid genome assemblies demonstrates the enduring quality of the reference assembly. Genome Res. 27 (5), 849–864. https://doi.org/10.1101/gr.213611.116.
Shah, R., Hinkle, C.C., Haris, L., Shah, R., Mehta, N.N., Putt, M.E., et al., 2012. Adipose genes down-regulated during experimental endotoxemia are also suppressed in obesity. J. Clin. Endocrinol. Metab. 97 (11), E2152–E2159. https://doi.org/10.1210/jc.2012-1988.
Shoelson, S.E., Lee, J., Goldfine, A.B., 2006. Inflammation and insulin resistance. J. Clin. Investig. 116 (7), 1793–1801. https://doi.org/10.1172/JCI29069.
Staiger, H., Tschritter, O., Machann, J., Thamer, C., Fritsche, A., Maerker, E., et al., 2003. Relationship of serum adiponectin and leptin concentrations with body fat distribution in humans. Obes. Res. 11 (3), 368–376. https://doi.org/10.1038/oby.2003.48.
Szklarczyk, D., Kirsch, R., Koutrouli, M., Nastou, K., Mehryary, F., Hachilif, R., et al., 2023. The STRING database in 2023: protein–protein association networks and functional enrichment analyses for any sequenced genome of interest. Nucleic Acids Res. 51 (D1), D638–D646. https://doi.org/10.1093/nar/gkac1000.
Tillaut, H., Monfort, C., Giton, F., Warembourg, C., Rouget, F., Cordier, S., et al., 2022. Persistent organic pollutant exposure and thyroid function among 12-year-old children. Neuroendocrinology 113 (12), 1232–1247. https://doi.org/10.1159/000528631.
Tontonoz, P., Spiegelman, B.M., 2008. Fat and beyond: the diverse biology of PPARgamma. Annu. Rev. Biochem. 77, 289–312. https://doi.org/10.1146/annurev.biochem.77.061307.091829.
Unal, R., Yao-Borengasser, A., Varma, V., Rasouli, N., Labbate, C., Kern, P.A., et al., 2010. Matrix metalloproteinase-9 is increased in obese subjects and decreases in response to Pioglitazone. J. Clin. Endocrinol. Metab. 95 (6), 2993–3001. https://doi.org/10.1210/jc.2009-2623.
Van Beek, L., Vroegrijk, I.O.C.M., Katiraei, S., Heemskerk, M.M., Van Dam, A.D., Kooijman, S., et al., 2015. F c R γ-chain deficiency reduces the development of diet-induced obesity. Obesity 23 (12), 2435–2444. https://doi.org/10.1002/oby.21309.
Villarroya, F., Giralt, M., Iglesias, R., 1999. Retinoids and adipose tissues: metabolism, cell differentiation and gene expression. Int. J. Obes. 23 (1), 1–6. https://doi.org/10.1038/sj.ijo.0800799.
Wang, B., Fu, X., Liang, X., Deavila, J.M., Wang, Z., Zhao, L., et al., 2017. Retinoic acid induces white adipose tissue browning by increasing adipose vascularity and inducing beige adipogenesis of pdgfrα+ adipose progenitors. Cell Discov. 3 (1), 1–14. https://doi.org/10.1038/celldisc.2017.36.
Wilcox, G., 2005. Insulin and insulin resistance. Clin. Biochem. Rev. 26 (2), 19–39.
Worldwide trends in body-mass index, underweight, overweight, and obesity from 1975 to 2016: a pooled analysis of 2416 population-based measurement studies in 128·9 million children, adolescents, and adults. Lancet (Lond. Engl.) 390 (10113), 2017, 2627–2642. https://doi.org/10.1016/S0140-6736(17)32129-3.